ACTA STEREOL 1991; 10/1: 113-122
ORIGINAL SCIENTIFIC PAPER

# EFFECTIVENESS OF STEEL WIRE REINFORCEMENT IN A BOUNDARY LAYER OF CONCRETE

Piet Stroeven

Stevin Laboratory, Faculty of Civil Engineering
Delft University of Technology, Stevinweg 4,
2628 CN Delft, The Netherlands

## ABSTRACT

External surfaces, such as those of the mold, exert influences on the orientation distribution of wires in concrete. Part of the influences is due to compaction leading to wire segregation in the mix. The influence is restricted to a boundary zone with a thickness of the same order of magnitude as wire length, i.e. about 50 to 60 mm. Experiments have revealed this zone mostly to be under-reinforced, while it only extended over about 50% of wire length.

Based on the concept of a partially-planar wire dispersion in bulk of the material, estimates are derived for orthogonal components of the reinforcement ratio (number of wires per unit of area, $N_A$) and of the tensile strength of the composite. To that end, wires violating the boundary conditions are not replaced in the model. The structural information is of a quasi-local nature, since properties are presented as a function of the depth under the surface.

Estimates for the reinforcement ratio of a boundary layer with a thickness of half the wire length correspond well to quantitative image analysis results obtained on about 300 section images of steel wire reinforced concrete (SWRC) containing volume fractions of wire varying between 0.5 and 3%. Similar data also resulted from a computer-simulation approach.

Keywords: Anisometry, anisotropy, boundary effect, steel wire reinforced concrete, structural modelling, reinforcement ratio.

## INTRODUCTION

A vast amount of experimental data form conclusive evidence for the existence of serious deviations of wire dispersion in SWRC from a state of "pure" randomness as generally assumed in constitutive modelling approaches. On a global level the reinforcement structure reveals anisometry and segregation. In materials testing it is nowadays well-accepted that such structural features can significantly influence mechanical properties. More recent investigations by Stroeven and Babut [1986] have additionally shown

Table 1. Wire efficiency for 2-D, 3-D and mixed systems

| 3-D | 2-D | Partially planar |
|---|---|---|
| $\eta_3 = \frac{1}{2}$ | $\eta_{2\parallel} = \frac{2}{\pi}$ | $\eta_\parallel = \frac{1}{2}[1 + (\frac{4}{\pi} - 1)\omega]$ |
| $\eta_3 = \frac{1}{2}$ | $\eta_{2\perp} = 0$ | $\eta_\perp = \frac{1}{2}(1 - \omega)$ |
| $\eta_{c3} = \frac{1}{3}$ | $\eta_{c2\parallel} = \frac{1}{2}$ | $\eta_{c\parallel} = \frac{1}{3}(1 + \frac{1}{2}\omega)$ |
| $\eta_{c3} = \frac{1}{3}$ | $\eta_{c2\perp} = 0$ | $\eta_{c\perp} = \frac{1}{3}(1 - \omega)$ |

boundary layers to be under-reinforced. Cracks will therefore meet here a relatively low resistance.

Estimates for wire anisometry and for anisotropic strength components in bulk of the material can be based on a partially (linear) planar wire system [Stroeven, 1989b]. This approach relies on a law of mixtures concept in which the wires contribute to the global mechanical properties in proportion to their volume fraction, $V_f$ , and to their orientation efficiency, $\eta$ . This can be formulated by

$$N_{A_\perp} = \eta_\perp L_V \tag{1}$$

$$N_{A_\parallel} = \eta_\parallel L_V \tag{2}$$

$$\sigma_{c\perp} = \sigma_m(1 - V_f) + \eta_{c\perp} a V_f \tau_f^* \tag{3}$$

$$\sigma_{c\parallel} = \sigma_m(1 - V_f) + \eta_{c\parallel} a V_f \tau_f^* \tag{4}$$

in which $a$, $L_V$ and $V_f$ are the aspect ratio, lineal and volume fraction of the wires, respectively. $\sigma$ defines a stress in concrete or mortar and $\tau_f^*$ is the intefacial friction resistance. In eqs (1) and (2) the reinforcement ratio's in orthogonal directions are governed by efficiency factors, $\eta_\perp$ and $\eta_\parallel$. These factors are proportional to the corresponding values of the average tangent height of the wires. The efficiency factors, $\eta_{c\perp}$ and $\eta_{c\parallel}$, in eqs (3) and (4) express the relative effectiveness of this anisometric wire system for stress transfer in orthogonal directions of a cracked SWRC material body.

These four efficiency factors combine in a linear way the contributions of the 2-D and 3-D systems in the partially planar reinforcement structure. Only in exceptional cases it seems worth to add a 1-D component to the model [Stroeven and Shah, 1978]. Table 1 presents the values for the efficiency factors of 2-D, 3-D and mixed systems. The relative contributions of the 2-D and 3-D systems to the mixed ones is reflected by the degree of orientation, $\omega$ , which is the ratio of 2-D to total fraction of wires.

The stereological concept underlying eqs (1) to (4) additionally asks for substitution of appropriate micromechanical characteristics in case of the strength problem. The given solutions are based on pull out and shearing over the crack edges of the wires intersecting with mesocracks in the material body. Further, at ultimate tensile strength (UTS) the shortest wire ends are supposed to be fully debonded during pulling out from the matrix. This is supported by experimental evidence coming from holographic interferometry studies [Bień and Stroeven, 1988]. The mono-sized wires can either be smooth-shaped, or provided with anchoring facilities. The most general case is presented in Stroeven [1989b].

The derivation of the efficiency factors can be visualized with the help of the so called "unit sphere model". In case of a IUR wire dispersion the sphere contains a normalized "random" set of such wires, joined at one end, while maintaining the wire

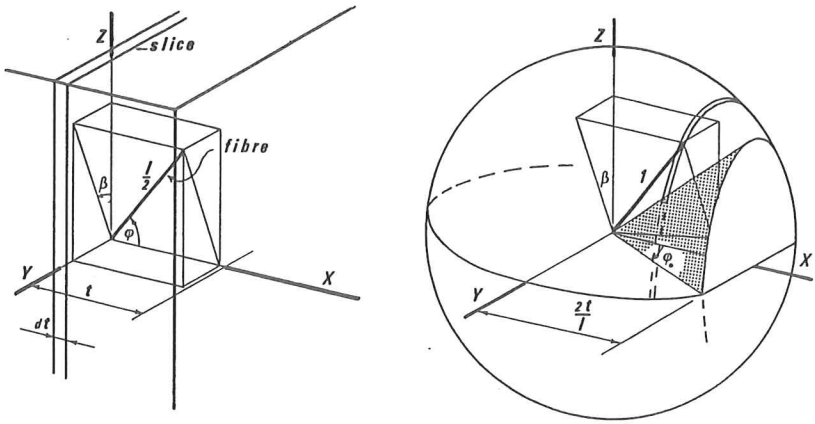


Fig. 1. Slice in the boundary zone (left) and associated unit sphere model with "empty" cone (right).

orientation in the dispersion. The surface of the sphere is covered uniformly at random by the free wire ends, as a consequence. The probability associated with intersection of wires and cracks is proportional to the sine of the enclosed angle. So the characteristics of wire orientation in the unit sphere have to be adjusted appropriately! Load transfer over the crack by such wires depends for pulling out on the cosine and for the shearing mechanism on the sine values of enclosed angles. These corrections have to be provided for in the unit sphere model in case of the derivation of strength estimates for bulk properties. The unit sphere model needs further adjustments upon approach of an external boundary. The solution of this problem will be pursued in what follows.

## MODELLING OF THE REINFORCEMENT STRUCTURE IN THE BOUNDARY ZONE

Structural elements in concrete technology have mostly plain boundaries. The boundary zone conceived in the modelling approach is therefore a part of the material body close to such a plain external surface. This boundary zone is imaginary sliced parallel to the external boundary. The slices are in the limiting case infinitely thin. Slices on the same depth under the surface, $t$, are jointly supposed to form a representative volume element (RVE). Global estimating is based on such RVE's. Structural parameters will be obtained as function of $t$, and are therefore of a quasi-local nature.

A section plane or crack surface perpendicular to the external surface intersects with the slices. This situation is sketched in fig. 1. The wires reinforcing the section or crack at the location of the slice are displayed in a unit sphere model. At positions remote from the external surface, the unit sphere model will be the one used for estimation of bulk properties. Upon approach of the boundary, some of the wire orientation will violate the boundary conditions. A methodological choise is required how to proceed from here on. Two procedures can be distinguished in wire processes to meet the requirements imposed by the boundary conditions. Either the rejected orientation can be replaced by a new randomly selected one, or location and orientation can be randomly re-established. The first situation leads to improved wire effectiveness in the boundary

zone, which would obviously conflict with experimental evidence. The second approach can be realized by taking a higher wire density in bulk. "Wires" in the unit sphere model violating boundary conditions in case of slices in the boundary zone are attributed a zero contribution. The complexity of the situation is coming from the fact that "violation" is resulting from "unfavourable" combinations of orientation and embedment depth (at crack or section).

## WIRE DENSITY IN THE BOUNDARY ZONE

Fig. 2 shows a cross section of the boundary zone perpendicular to the external surface. The intersection line with the section plane or crack surface coincides with the $x$-axis. The slice is situated on a distance $t$ from the external surface. Wires in the plane of the cross section are considered. Next, the cross sectional plane is rotated over an angle $\beta$, whereupon the study of the reinforcement characteristics is continued.

Three domains can be distinguished. For larger values of the sharp angle $\phi$, enclosed by wire and $x$-axis the boundary conditions do not impose any restrictions on wire density. This is DOMAIN I. For $\alpha = \phi$ with $\cos\alpha = t/l$ ($l$ being wire length) DOMAIN II sets in. For smaller values of $\phi$ some of the wires in the given direction will violate the boundary condition, and will be "removed" from the model. Such wires have their shortest embedded length "below" the $x$-axis (the section or crack plain). Wire density in the given direction within DOMAIN II is reduced with decline in angle $\phi$, as a consequence.

DOMAIN III stretches from $\phi = 0$ to $\phi = \gamma$, with $\cos\gamma = 2t/l$. In addition to all wires having their shortest embedded length below the $x$-axis, also some having their shortest embedded length above it have to be "removed". Wire density, after staying constant in domain I, will therefore gradually decline over domains II and III. It can easily be seen from fig. 2 that the decline is proportional to $\cos\alpha/\cos\phi$.

Upon integration over $\beta$ the wire density (number of wires per unit of volume) is obtained as function of slice location, $t$. Hence,

$$\begin{aligned} N_V(\alpha) &= \frac{2}{\pi} N_V \left[ \int_0^{\pi/2} \int_0^{\pi/2} \sin\phi \, d\phi \, d\beta + \int_0^{\pi/2} \int_0^{\alpha} \sin\phi \frac{\cos\alpha}{\cos\phi} d\phi \, d\beta \right] \\ &= N_V \left[ \cos\alpha - \cos\alpha \ln\cos\alpha \right] = \varsigma N_V \end{aligned} \tag{5}$$

in which $\cos\alpha = t/l$. In bulk $\alpha = 0$ (and $t \geq l$), so that eq (5) correctly degenerates into a trivial expression. Wire density will be zero at the external surface, where $t = 0$.

Fig. 3 more precisely shows the decline in wire density over the boundary zone when moving outwards with the slice. The major part of the reduction in wire density occurs over a boundary layer with a thickness of half the wire length. Average wire density over this layer amounts to 0.55 of its bulk value. A dashed line indicates the approximation of a material body having such a boundary layer with a smeared out wire density and a unit bulk wire density in the residual portion.

## REINFORCEMENT RATIO IN THE BOUNDARY LAYER

The reinforcement ratio in the boundary layer is governed by the average tangent height, $\overline{H}$, of the wires. The projected length of a wire from a 3-D system is $l \sin\phi \cos\beta$,

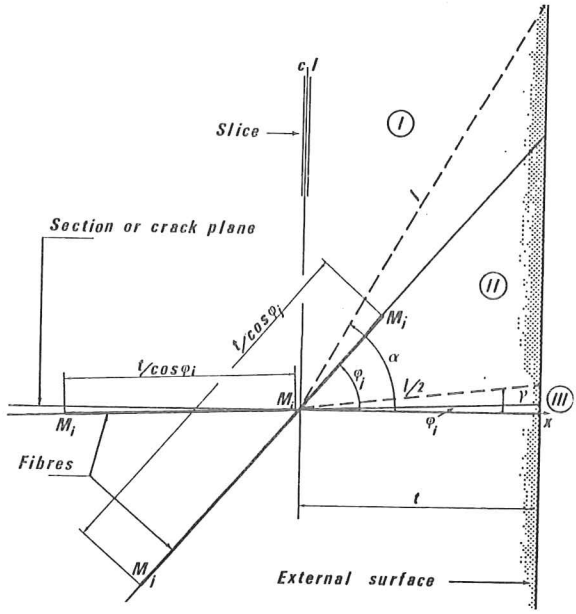


Fig. 2. Cross-section of boundary zone perpendicular to external surface through wire/fibre reinforcing slice at $x$-axis.

as can be see in fig. 1. In analogy with the integral expressions of eq (5), the efficiency factor, $\eta_3$ , defined by $\overline{H} = \eta_3 l$, is given by

$$\begin{aligned}\eta_3 &= \frac{\int_0^{\pi/2}\int_\alpha^{\pi/2} \sin^2\phi\cos\beta\, d\phi d\beta + \int_0^{\pi/2}\int_0^{\alpha} \frac{\cos\alpha}{\cos\phi} \sin^2\phi\cos\beta\, d\phi d\beta}{\int_0^{\pi/2}\int_0^{\pi/2} \sin\phi\, d\phi d\beta} \\ &= \frac{2}{\pi}\cos\alpha \ln\tan\left(\frac{\alpha}{2}+\frac{\pi}{4}\right) - \frac{1}{2\pi}\sin 2\alpha + \frac{1}{2} - \frac{\alpha}{\pi} \qquad (6)\end{aligned}$$

For $\alpha = 0$ and $\alpha = \pi/2$ eq (6) leads to the correct limiting values, i.e. 0.5 and 0, respectively (viz. Table 1). $\eta_3$ is also plotted in fig. 3.

Anisometry of a partially planar wire composite can be expressed by the orthogonal components of the reinforcement ratio. Hence,

$$N_{A\parallel} = \eta_3 L_{V3} + \frac{2}{\pi} L_{V2} \qquad (7)$$

$$N_{A\perp} = \eta_3 L_{V3} \qquad (8)$$

and upon substitution of the degree of orientation,

$$N_{A\parallel} = L_V\{\frac{2}{\pi}\omega + \eta_3(1-\omega)\} = \eta_\parallel L_V \qquad (9)$$

$$N_{A\perp} = L_V \eta_3(1-\omega) = \eta_\perp L_V \qquad (10)$$

Eqs (9) and (10) present estimates of the othogonal components of the reinforcement ratio as function of the depth under the surface of the material body. For a boundary

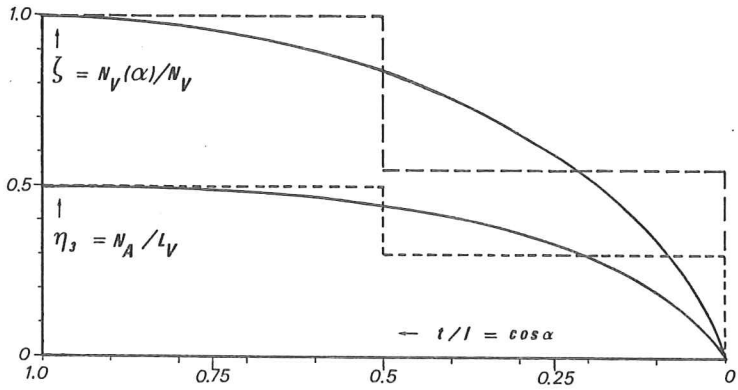


Fig. 3. Decline over the boundary zone in efficiency factors related to wire density ($N_V$) and to reinforcement ratio ($N_A$).

zone with a thickness of half the wire length smeared out values for the efficiency factors, $\eta_\parallel$ and $\eta_\perp$, of 0.4 and 0.2 are found, under the assumption of a degree of orientation around 0.3. Even when stressed in the direction of the orientation plane of the 2-D component the reinforcement efficiency will be significantly reduced. On the average it will amount to 70% when compared to its bulk features and to 80% when compared with those of a hypothetical 3-D system (commonly used as reference in the design).

It should finally be noted that eq (6) contains the effect of declining wire density as given by eq (5). The ratio of both expressions therefore yields the average tangent height of wires with unit length present in the boundary zone. It can easily be seen, that in the interior $\overline{H}/l = 1/2$ and at the exterior $\overline{H}/l = 2/\pi$; close to the external surface the wires can only be dispersed parallel to this plane.

## WIRE EMBEDMENT LENGTH IN THE BOUNDARY ZONE

Fig. 2 was used to demonstrate the reduction in wire density with wire orientation. Systematic removal of wires from the model also affects the wire embedment length, $l_e(\phi,\beta)$, of course. Simple mathematical manipulation allows deriving the following expressions for the average embedment length in the three successive domains

$$l_e(\phi,\beta) = \frac{l}{4} \tag{11}$$

$$l_e(\phi,\beta) = \frac{l}{4}(-1 + 4\frac{\cos\alpha}{\cos\phi} - 2\frac{\cos^2\alpha}{\cos^2\phi}) \tag{12}$$

$$l_e(\phi,\beta) = \frac{l}{4}(2\frac{\cos^2\alpha}{\cos^2\phi}) \tag{13}$$

Analogously with the foregoing, eqs (11) to (13) can be averaged over all possible angles. It should be noted, that for locations of the slice up to a depth of half the fibre length all three domains have a finite extension. It can easily be shown, that $l_e(\alpha)$ for such positions is given by [Stroeven, 1989a], noting that $\cos\gamma = 2\cos\alpha$

$$l_e(\alpha) = \frac{l}{4}\{1 + \frac{2}{\pi}\gamma - \frac{4}{\pi}\alpha - \frac{10}{\pi}\sin 2\alpha - \frac{1}{\pi}\sin 2\gamma + \frac{16}{\pi}\cos\alpha \ln\left[2\frac{1+\sin\alpha}{1+\sin\gamma}\right] +$$

$$+\frac{16}{\pi}\cos^2\alpha\tan\gamma+\frac{16}{\pi}\cos\alpha\sin\gamma+\frac{8}{\pi}(\alpha-2\gamma)\cos^2\alpha\} \quad (14)$$

For positions of the slice in the boundary zone more remote from the external surface domain III is non-existent. In this case the average embedment length will amount to [Stroeven, 1989b]

$$l_e(\alpha)=\frac{l}{4}\{1-\frac{4}{\pi}\alpha-\frac{10}{\pi}\sin 2\alpha+\frac{16}{\pi}\cos\alpha\ln\frac{1+\sin\alpha}{\cos\alpha}+\frac{8}{\pi}\cos^2\alpha\} \quad (15)$$

Eqs (14) and (15) yield for the exterior and interor the correct values, i.e. zero and $l/4$. Halfway the boundary zone the two expressions both lead to a value for $l_e(\alpha)$ of $0.93(l/4)$, which again demonstrates the major part of the decline in reinforcement characteristics to take part in a layer of half the wire length. It should be noted, that expressions (14) and (15) contain the reduction in wire density in the boundary zone.

## STRENGTH OF THE BOUNDARY LAYER

The main wire contribution to strength is due to the stress transmitted perpendicularly to the crack plane. The stress component is proportional to the product of the average projected embedment length (= embedment depth) and the number of wires. The integration procedure is similar as in case of the derivation of eqs (14) and (15). An extra projection factor is added, which is proportional to $\sin\phi\cos\beta$. The strength efficiency factor, $\eta_{c3}$, is in the case of three finite domains given by

$$\begin{aligned}\eta_{c3} &= \frac{\frac{1}{2}\int_0^{\pi/2}\int_0^{\gamma}\frac{\cos^2\alpha}{\cos^2\phi}\sin^3\phi\cos^2\beta\,d\phi d\beta+\int_0^{\pi/2}\int_\gamma^{\alpha}(\frac{\cos\alpha}{\cos\phi}-\frac{1}{4}-\frac{\cos^2\alpha}{\cos^2\phi})\sin^3\phi\cos^2\beta\,d\phi d\beta}{\int_0^{\pi/2}\int_0^{\pi/2}\sin\phi\,d\phi d\beta}+\\ &+\frac{\frac{1}{4}\int_0^{\pi/2}\int_0^{\pi/2}\sin^3\phi\cos^2\beta\,d\phi d\beta}{\int_0^{\pi/2}\int_0^{\pi/2}\sin\phi\,d\phi d\beta}\\ &= \cos^3\alpha-2\cos^2\alpha+2\ln 2\cos\alpha \end{aligned} \quad (16)$$

For slices in the boundary zone more remote from the external surface it can easily be shown that

$$\eta_{c3}=-\frac{1}{3}\cos^3\alpha+2\cos^2\alpha-\cos\alpha-2\cos\alpha\ln\cos\alpha-\frac{1}{3} \quad (17)$$

Eqs (16) and (17) yield correct values in the interior (1/3) and at the exterior surface (zero) (viz. Table 1). Halfway the boundary zone a common value of $0.95(1/3)$ is found. The smeared out strength value for a boundary zone with a thickness of half the wire length is $0.64(1/3)$. For details, see [Stroeven, 1989a].

## REDUCED STRENGTH OF THE BOUNDARY ZONE

Eqs (3) and (4) can more accurately be specified for a partially planar composite in which account is given to stress transfer at cracks by wire pull out and by shearing of the wires over the crack edges. Also the wires could be provided with anchoring facilities operating as ploughs [Stroeven, 1989b]. Hence,

$$\sigma_{c\|} = \sigma_m(1-\varsigma V_f)+aV_f\tau_f^*(\eta_{c3}+[\frac{1}{2}-\eta_{c3}]\omega) \quad (18)$$

$$\sigma_{c\perp} = \sigma_m(1-\varsigma V_f)+aV_f\tau_f^*\eta_{c3}(1-\omega) \quad (19)$$

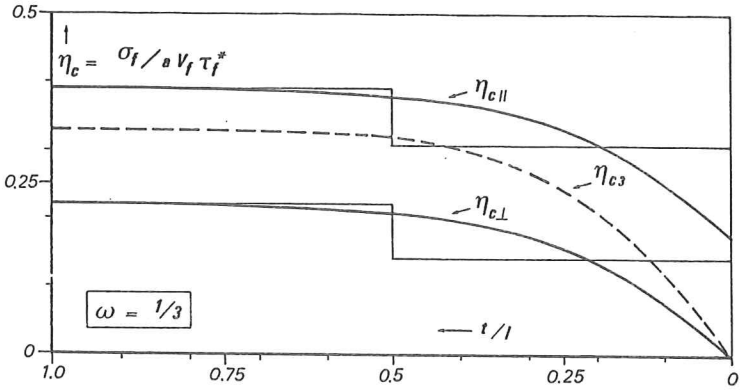


Fig. 4. Decline over the boundary zone of orthogonal tensile strength components of a partially planar wire composite.

It can be concluded from a comparison of eqs (3) and (4) on the one hand, and eqs (18) and (19) on the other hand, that the orthogonal components of the efficiency factors of a partially planar system are given by

$$\eta_{c\|} = (\eta_{c3} + [\frac{1}{2} - \eta_{c3}]\omega) \tag{20}$$

$$\eta_{c\perp} = \eta_{c3}(1 - \omega) \tag{21}$$

For a 3-D ($\omega = 0$) and a 2-D composite ($\omega = 1$) eqs (20) and (21) yield the correct values, as can easily be verified (viz. Table 1).

Expressions (18) and (19) for the strength components can be averaged over a boundary zone with a thickness of half the wire length [Stroeven, 1989a].

$$\overline{\sigma}_{c\|} \simeq \sigma_m(1 - 0.55V_f) + 0.21aV_f\tau_f^*(1 + \frac{4}{3}\omega) \tag{22}$$

$$\overline{\sigma}_{c\perp} \simeq \sigma_m(1 - 0.55V_f) + 0.21aV_f\tau_f^*(1 - \omega) \tag{23}$$

The wire contributions to UTS of the composite turn out to be twice as large in the direction of the orientation plane of the 2-D portion as it is in a direction orthogonal to this plane, provided $\omega$ is around 0.3!

Dividing expressions (22) and (23) by the appropriate expressions for the anisotropic strength components in bulk allows assessing the components of the relative strength decline in the boundary layer, $R_{\|}$ and $R_{\perp}$.

$$R_{\|} = \frac{1 + 0.21A(1 + \frac{4}{3}\omega)}{1 + 0.33A(1 + \frac{1}{2}\omega)} \tag{24}$$

$$R_{\perp} = \frac{1 + 0.21A(1 - \omega)}{1 + 0.33A(1 - \omega)} \tag{25}$$

in which $A = (aV_f\tau_f^*)/(\sigma_m[1 - \frac{1}{2}V_f])$.

For prismatic wires without anchoring facilities a value of $A$ was found of about 6 [Stroeven, 1989a]. This will be higher when wires are provided with anchoring facilities, of course. For a value of 10 eq (25) estimates a strength reduction by 25% for $\omega = 1/3$. This is a relevant situation in case of spalling off risk due to reinforcement corrosion.

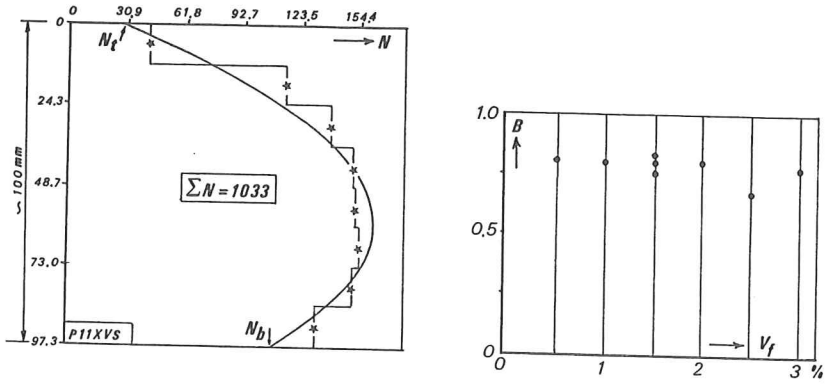


Fig. 5. Distribution of wires over vertical cross-section of SWRC (left) and boundary effect, $B$, for different mixes of SWRC.

## EXPERIMENTAL

The international literature offers limited experimental data pertaining to the actual state of wire distribution in cementitious composites. Still it is widely recognized nowadays that segregation and partial orientation in the reinforcement structure are the inevitable results of material production in general and of compaction in particular; density and degree of orientation increase toward the bottom side of structural elements. Hence, the orthogonal components of the efficiency factors, $\eta_{\|}$, and $\eta_{\perp}$, defined in eqs (9) and (10), are in the same direction also changing. Segregation will be the dominant factor as can be seen in fig. 5. This figure is taken from an extensive investigation of mechanical proporties and structural characteristics of SWRC specimens containing up to 3 volume percent of wires. Details are given in Stroeven and Babut [1986] and Stroeven [1987].

The aforementioned study encompassed about 300 analysed cross-sections of specimens. The image patterns were oriented in either one of the Cartesian coordinate directions. The coordinates of the wire sections were recorded by a Quantimet 720. This allowed to analyse the distribution of $N_A$ in a particular direction by defining narrow (strip-like) fields covering the image plane. This forms the basis for the data plotted in fig. 5 at the right. The fields had a width of half the wire length (12.5 mm).

Apart from revealing segregation in the direction of the gravity field, it becomes clear from fig 5, that external layers were under-reinforced. This is quantified by a factor $B$ (=boundary effect), defined as $(N_t + N_b)/2\overline{N}$. Herein, the successive symbols refer to the wire density in the *t*op field, in the *b*ottom field, and in the cross-section. Group averages (for all similarly oriented sections of 6 specimens sawn from one plate) of $B$ are plotted in fig 5. It should be noted, that the value of $B$ for a section perpendicular to the gravitational direction will slightly exceed the value of $\eta$. It can easily be seen from its definition that an experimental value of 0.8 for $B$ (reflected by fig 5) would correspond to a value of 0.75 for $\eta_{\|}$, provided $\omega$ is around 0.3. This experimental value corresponds to the estimated one (i.e. 0.74)!

The efficiency factor, $\eta_{3\|}$, was also studied with the help of a computer simulation system. Details are given by Guo and Stroeven [1989]. For mixes with a volume fraction of wires between 0.5 and 1.5 this efficiency factor varied between 0.56 and 0.58, which confirms the theoretical set up as well.

## CONCLUSIONS

It is outlined how the effectiveness of wire reinforcement in boundary layers of cementitious composites can be obtained by applying stereological notions. The model is based on a partially-planar wire system of which the orientation plane is parallel to one of the external surfaces of the material body. Estimation of ultimate strength relies on a law of mixtures concept. The shortest embedded parts of wires inhibiting crack growth are assumed completely debonded from the matrix, so that they will be pulled out from the matrix pockets and sheared over the crack edges. The wires in the IUR portion of the wire system which are violating the boundary conditions in the vicinity of external surfaces of the material body are removed from the model.

It is shown that for engineering purposes the disturbaces in the reinforcement structure can be restricted to a layer with a thickness of half the wire length. Estimates for orthogonal efficiency components of the reinforcemnent ratio are derived. Outcomes are supported by experimental evidence. Estimates for orthogonal effciency components of wire contributions to UTS are additionally derived. Significant loss of strength capacity in the external part of the boundary layer should be considered in crack development studies. Obtained results have also relevance for estimating the efficiency of wire additions for reducing spalling risk due to corrosion of the main reinforcement in structural elements.

## REFERENCES

Bień J, Stroeven P. Holographic interferometry study of debonding between steel and concrete. In: Engineering Applications of New Composites. Eds. Paipetis SA, Papanicolaou GC. Wallingford: Omega Scientific, 1988: 213-8.

Guo W, Stroeven P. The analysis of wire distributions in computer-simulated wire reinforced materials. Acta Stereol, 1989; 8: 683-8.

Stroeven P. Research strategy for steel fibre reinforced concrete. Acta Stereol, 1987; 6/III: 555-60.

Stroeven P. Boundary effects in fibre reinforced composites. Report 25-89-01, Faculty of Civil Engineering, Delft University of Technology, 1989a.

Stroeven P. Structural characterization of steel fibre reinforced concrete. In: Brittle Matrix Composites 2. Eds. Brandt AM, Marshall IH. London: Elsevier Appl Sc, 1989b: 34-43.

Stroeven P, Babut R. Structural variations in steel fibre reinforced concrete and its implications for material behaviour. In: Brittle Matrix Composites 1. Eds. Brandt AM, Marshall IH. London: Elsevier App Sc, 1986: 421-34.

Stroeven P, Shah SP. Use of radiography-image analysis for steel fibre reinforced concrete. In: Testing and Test Methods of Fibre Cement Composites. Ed. Swamy RN. Lancaster: The Constr Press, 1978: 275-88.

Received: 1991-03-26 Accepted: 1991-06-18